New Mechanistic Insights into the Iridium – Phosphanooxazoline-Catalyzed Hydrogenation of Unfunctionalized Olefins: A DFT and Kinetic Study

Peter Brandt,*[a] Christian Hedberg,[b] and Pher G. Andersson[b]

Abstract: The reaction mechanism of the iridium – phosphanooxazoline-catalyzed hydrogenation of unfunctionalized olefins has been studied by means of density functional theory calculations (B3LYP) and kinetic experiments. The calculations suggest that the reaction involves an unexpected $Ir^{III}-Ir^{V}$ catalytic cycle facilitated by coordination of a second equivalent of dihydrogen. Thus, in the rate-determining migratory insertion of the substrate alkene into an iridium – hydride bond, simultaneous oxidative addition of the bound dihydrogen occurs. The kinetic data shows that the reaction is first order with respect to hydrogen pressure. This is interpreted in terms of an endergonic coordination of this second equivalent of dihydrogen, although a rate-determining step, in which coordinated solvent is replaced by dihydrogen, could not be ruled out. Furthermore, the reaction was found to be zeroth order with respect to the alkene concentration. This correlates well with the calculated exothermicity of substrate coordination, and the catalyst is thus believed to coordinate an alkene in the resting state. On the basis of the proposed catalytic cycle, calculations were performed on a full-sized system with 88 atoms to assess the appropriateness of the model calculations. These calculations were also used to explain the enantioselectivity exerted by the catalyst.

Keywords: asymmetric catalysis · density functional calculations · hydrogenation · iridium · kinetics

Introduction

An efficient method for enantioselective hydrogenation of unfunctionalized olefins has recently been developed by Pfaltz.[1, 2] These catalytic systems are based on the discovery made by Crabtree and co-workers,[3] that the $[Ir(cod)PCy_3(pyridine)][PF_6]$ (cod = cyclooctadiene) complex is a remarkably efficient catalyst for the hydrogenation of tri- and even tetrasubstituted unfunctionalized olefins. The presence of COD in the precatalyst assures irreversible formation of free coordination sites at the metal. Thus, in the activation of the catalyst, this ligand is reduced and cyclooctane is released. Several studies have been devoted to the understanding of this process and the oxidative addition of H_2 to Ir – cod complexes is known in some detail.[4] However, the knowledge of the real catalyst and the exact mechanism for the hydrogenation of olefins is very limited. To increase the understanding of this reaction, we have performed a hybrid density functional study (B3LYP) that covers a large range of the potential intermediates and transition states in the reaction. We have also carried out a kinetic study to gain additional support for the conclusions drawn from the density functional theory calculations. Herein, we propose a reaction mechanism that agrees with previously reported experimental findings, and which could be used to rationalize the enantioselectivity in the hydrogenation of tri- and tetrasubstituted olefins.

[a] Dr. P. Brandt
Department of Structural Chemistry
Biovitrum AB, S-11276 Stockholm (Sweden)
Fax: (+46) 8-697-23-19
E-mail: peter.brandt@biovitrum.com

[b] C. Hedberg, Prof. Dr. P. G. Andersson
Department of Organic Chemistry, Uppsala University
Box 531, S-75121 Uppsala (Sweden)
Fax: (+46) 18-51-25-24
E-mail: phera@akka.kemi.uu.se

Computational Methods

Model system: Because of the large number of configurationally different iridium complexes possible in this reaction, a model of reduced size had to be used in the initial DFT study. This model was constructed from the phosphanooxazoline ligand developed by Pfaltz (Scheme 1): the oxazoline moiety was replaced by an *N*-methyl imine functionality and the triarylphosphine by a dimethylvinylphosphine moiety (Scheme 2). As a substrate, we used ethylene as a substitute for the experimentally more commonly used substituted styrenes.

Formation of the active catalyst takes place by an irreversible hydrogenation of the ligand cyclooctadiene and displacement of the alkane product by either solvent, dihydrogen, or a substrate alkene. As a starting point for our calculations, we selected ten isomers, denoted **A**-H_2 to **F′**-H_2,

  0947-6539/03/0901-0339 $ 20.00+.50/0

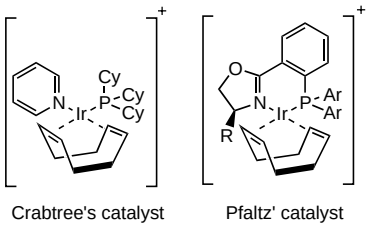

Scheme 1. Iridium pre-catalysts developed by Crabtree and Pfaltz.

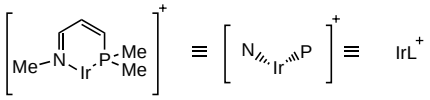

Scheme 2. Simplified model system used in the calculations and abbreviations used in the following text and figures.

of a dihydrido hydrogen ethylene complex of iridium(III). The configurations of these isomers are depicted in Scheme 3. Removal of H_2 from these complexes generated new reaction paths referred to as **A**–**F′**. We have arbitrarily selected the most stable $[IrL(H)_2(CH_2Cl_2)_2]^+$ complex, namely **1**, (Figure 1) as a reference point of all energies throughout this manuscript.

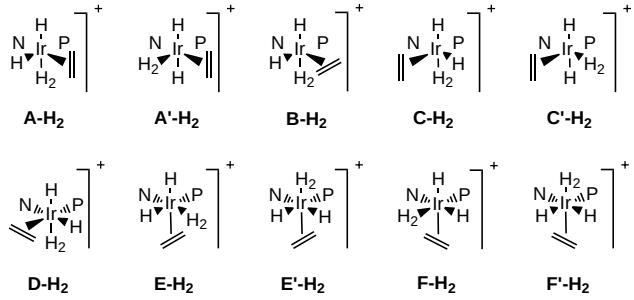

Scheme 3. The ten different starting configurations examined.

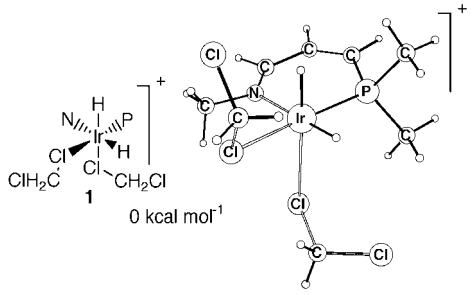

Figure 1. The energetic reference point used throughout this work.

Density functional theory calculations: All geometry optimizations as well as final energy determinations were performed with the B3LYP[5] hybrid density functional. The study was made in several consecutive steps starting with a screening of a large range of possible reaction paths. In this initial study, geometries and energies were calculated with the Gaussian 98 program[6] and the double-ζ quality LANL2DZ basis set.[7] This implies the use of effective core potentials for 10 and 60 core electrons of phosphorus and iridium, respectively. The LANL2DZ basis set involves the use of d95v for C, N, O, and H; and a (5s, 6p, 3d) primitive basis contracted to [3s, 3p, 2d] for Ir. For phosphorus, a (3s, 3p) primitive basis contracted to [2s, 2p] was used. This basis set will be referred to as BS I throughout this work.

The routes lowest in energy were further evaluated by determining Hessians and zero-point corrections at the same level of theory. Final energies were determined with the SDD[8] basis set and a quasirelativistic effective core potential for iridium, replacing 60 core electrons. The SDD basis set for Ir uses a (8s, 7p, 6d) primitive basis contracted to [6s, 5p, 3d]. This basis set was augmented by one f-polarization function with an exponent of 0.65. For other atoms, 6–311 + G** was used. This basis set combination will be referred to as BS II in the following.

After these first two steps, the steric influence on the paths lowest in energy was evaluated. This was carried out by means of the methods described above with 2-methyl-2-butene as the substrate.

The final geometry optimizations were carried out on a full-sized Pfaltz' catalyst (R = *t*Bu, Ar = Ph, Scheme 1) with (*E*)-1,2-diphenylpropene as the substrate. The three distances between Ir, the leaving hydride, and the Ir-bound carbons of the ethylene moiety were constrained to the distances found in the transition state for migratory insertion in path **C**-H_2, and the resulting structure was optimized in the Jaguar program[9] with B3LYP and the LACVP basis set keyword. LACVP refers to the use of LANL2DZ for Ir, as described above, and the 6-31G basis set for other atoms. Thereafter, a nonconstrained transition state search was performed by means of the quadratic synchronous transit (QST) method. Flanking π-alkene and alkyl intermediates were also fully optimized without constraints as well as the full version of complex **1** (Figure 1) and an intermediate $[Ir^{III}L(H)_2(CH_2Cl_2)$-(alkene)] complex.

Kinetics: In order to differentiate among the mechanistic alternatives, we derived an expression for the relative rates between different reaction pathways based on the calculated barrier for migratory insertion and reductive elimination. The underlying mechanistic basis assumes a common resting state of the catalyst, a semireversible formation of the Ir–ethyl complex (**3**), present in a steady-state concentration, and an irreversible reductive elimination according to Figure 2.

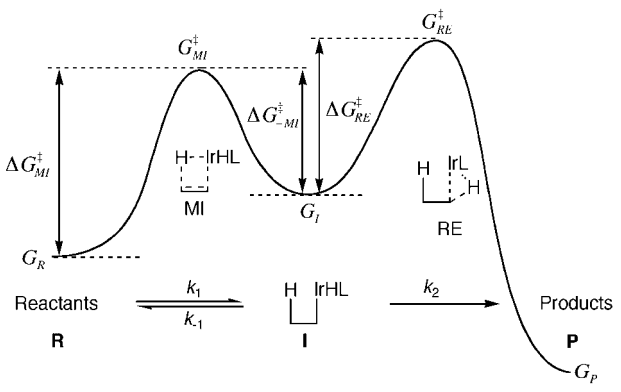

Figure 2. Mechanistic basis for the derivation of relative rates.

0947-6539/03/0901-0340 $ 20.00+.50/0 *Chem. Eur. J.* **2003**, *9*, No. 1

The kinetic expressions can now be written as Equations (1) and (2):

$$\frac{\partial[\mathrm{R}]}{\partial t} = -k_1[\mathrm{R}] + k_{-1}[\mathrm{I}] \quad (1)$$

$$\frac{\partial[\mathrm{I}]}{\partial t} = k_1[\mathrm{R}] - k_{-1}[\mathrm{I}] - k_2[\mathrm{P}] \quad (2)$$

in which [R] is the concentration of the olefin, [I] is the concentration of the intermediate iridium complex, and [P] is the concentration of the alkane product.

Under steady-state conditions [Eq. (3)], Equation (4) can be derived from Equations (2) and (3) and Equation (5) from Equations (1) and (4):

$$\frac{\partial[\mathrm{P}]}{\partial t} = -\frac{\partial[\mathrm{R}]}{\partial t}; \frac{\partial[\mathrm{I}]}{\partial t} = 0 \quad (3)$$

$$[\mathrm{I}] = \frac{k_1[\mathrm{R}]}{k_{-1} + k_2} \quad (4)$$

$$\frac{\partial[\mathrm{R}]}{\partial t} = -k_1[\mathrm{R}] + k_{-1}\frac{k_1[\mathrm{R}]}{k_{-1} + k_2} \quad (5)$$

Equation (5) then rearranges to Equation (6):

$$\frac{\partial[\mathrm{R}]}{\partial t} = [\mathrm{R}]\left(\frac{k_1 k_{-1}}{k_{-1} + k_2} - k_1\right) = -[\mathrm{R}]\left(\frac{k_1 k_2}{k_{-1} + k_2}\right) \quad (6)$$

Inserting $k_1 = ce^{-\Delta G_{\mathrm{MI}}/RT}$, $k_{-1} = ce^{-\Delta G_{-\mathrm{MI}}/RT}$, and $k_2 = ce^{-\Delta G_{\mathrm{RE}}/RT}$, in which $\Delta G^{\ddagger}_{\mathrm{MI}}$, $\Delta G^{\ddagger}_{-\mathrm{MI}}$, and $\Delta G^{\ddagger}_{\mathrm{RE}}$ are defined as in Figure 2, and $c = kT/h$ results in Equations (7), and finally Equation (8) for the rate:

$$\frac{\partial[\mathrm{R}]}{\partial t} = -c[\mathrm{R}]\left(\frac{e^{-\Delta G_{\mathrm{MI}}/RT}\, e^{-\Delta G_{\mathrm{RE}}/RT}}{e^{-\Delta G_{-\mathrm{MI}}/RT} + e^{-\Delta G_{\mathrm{RE}}/RT}}\right) = -c[\mathrm{R}]\left(\frac{e^{-(G_{\mathrm{MI}} - G_{\mathrm{R}})/}\, e^{-(G_{\mathrm{RE}} - G_1)/RT}}{e^{-(G_{\mathrm{MI}} - G_1)/RT} + e^{-(G_{\mathrm{RE}} - G_1)/RT}}\right) \quad (7)$$

$$\frac{\partial[\mathrm{R}]}{\partial t} = -c[\mathrm{R}]\left(\frac{e^{-(G_{\mathrm{MI}} - G_{\mathrm{R}} + G_{\mathrm{RE}})/RT}}{e^{-(G_{\mathrm{MI}})/RT} + e^{-(G_{\mathrm{RE}})/RT}}\right) \quad (8)$$

It is evident from Equation (8) that, within the limits of the approximations, the rate of the reaction is independent of the absolute energy of the intermediate iridium–alkyl complex and that relative rates between different reaction pathways of equal molecularity are independent of the energy of the resting state of the catalyst. An endergonic addition of H_2 to the postulated resting state iridium–dihydrido complex would lead to a first-order dependence on the hydrogen pressure. Similarly, endergonic addition of alkene would lead to a first-order dependence on substrate concentration.

Results

Potential energy surfaces: The steps evaluated are the coordination of ethylene and H_2 to **1** by solvent displacement, the transition state for migratory insertion (**TS**$_{(2\rightarrow3)}$) that generates an iridium–ethyl complex **3**, and the subsequent transition state for reductive elimination (**TS**$_{(3\rightarrow4)}$). The species studied is schematically drawn in Scheme 4, and the potential energies of each reaction pathway is reported in Table 1.

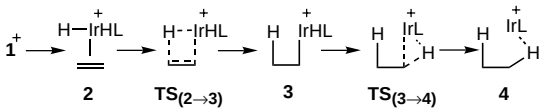

Scheme 4. Intermediates and transition states evaluated.

Table 1. Potential energies [kcal mol^{-1}] derived from B3LYP/BSI.

Path	**2**	**TS**$_{(2\rightarrow3)}$	**3**	**TS**$_{(3\rightarrow4)}$	log(rel. rate)[a]
A	1.9	15.1	7.9	19.2	0
A′	14.3	21.5	5.0	–	–
B	−2.4	5.6	0.3	12.9(8.9)[b]	4.6
C	0.4(−10.4)[b, c]	15.5	1.3	12.9	2.7
C′	26.8	34.4	16.5	–	–
D	−1.6	5.7	4.5	19.2(14.9)[b]	0
E’-S[d]	−1.9	0.7	−10.2	8.6	**7.8**
A-H_2	−9.1	6.0	−8.8	−7.6	**9.7**
A′-H_2	−3.1	8.4	−7.5	–	–
B-H_2	−11.6	−3.4	−8.0	5.6	**10.0**
C-H_2	−11.3	1.7	−9.7	−9.0	**12.9**
C′-H_2	−5.0	5.8[e]	−9.7	−9.0	9.9
D-H_2	−10.9	−2.8	−4.2	11.9	5.4
E-H_2	−9.1	6.1[f]	−8.8	3.5	9.6
E′-H_2	−4.8	−0.8	−8.8	3.5	**11.6**
F′-H_2	−3.4	2.7	−1.0	12.7	4.8
F-H_2	−7.5	[c]	–	–	–

[a] The relative rates are directly based on energies without thermal correction to enthalpies or zero-point corrections. The underlying mechanistic basis assumes a common resting state of the catalyst, a semi-reversible formation of the Ir–ethyl complex **3** present in a steady-state concentration, and an irreversible reductive elimination. Values in bold type indicate the paths that were subjected to further calculations. [b] Adding CH_2Cl_2 to the free coordination site. [c] The corresponding alkyl complex is a nonstationary point and optimizes back to the alkene complex. [d] With an axially coordinated dichloromethane molecule added to stabilize the equatorial arrangement of the hydrides. [e] This transition state leads to the same iridium-ethyl complex as path **C**-H_2. [f] This transition state leads to the same iridium-ethyl complex as path **E′**-H_2.

Kinetics: Two different sets of experiments were performed and every data point was run in duplicate. Firstly, a series of reactions were run at 10 bar hydrogen pressure with 0.5 mmol of (*E*)-1,2-diphenylpropene as the substrate and 0.5 mol% of catalyst in 1, 2, 3, and 4 mL of dichloromethane. This resulted in a first-order dependence on catalyst concentration (Figure 3) and a zeroth-order dependence in substrate concentration, as indicated by the conversion-independent rates.

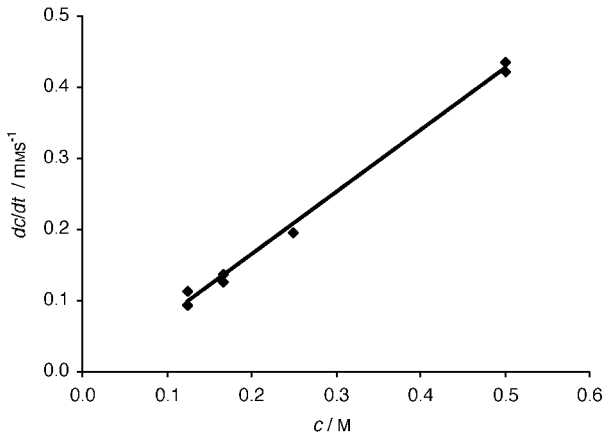

Figure 3. Observed rate of the reduction vs. concentration of catalyst (slope = 0.877, intercept = 0.0120, $r^2 = 0.996$).

  0947-6539/03/0901-0341 $ 20.00+.50/0

In the second experiment, 0.5 mmol of (*E*)-1,2-diphenylpropene was reduced at hydrogen pressures of 2, 4, 6, and 8 bar with 0.5 mol% of catalyst in 2 mL of dichloromethane. This revealed a first-order dependence on the hydrogen pressure (Figure 4).

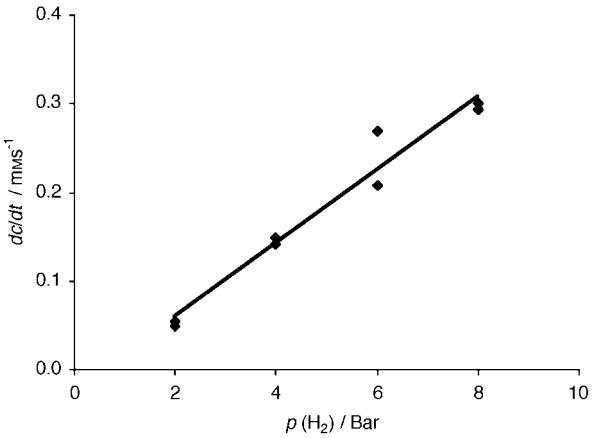

Figure 4. Observed rate of the reduction vs. hydrogen pressure (slope = 0.0414, intercept = 0.0243, $r^2 = 0.963$).

Discussion

To compute reaction mechanisms in advance of, or at least concomitantly with, the experiments is one of the ultimate goals of computational chemistry. In this study, we have made an extensive computational screening of possible intermediates and transition states in a very complicated reaction. From these calculations, based on a simplified model system, a complex picture of the iridium-catalyzed hydrogenation of alkenes has emerged. By the use of this approach, several mechanistic pathways could be excluded whereas other routes turned out to be more advantageous. The discussions are divided into six consecutive parts: 1) initial screening of possible reaction paths, 2) more accurate calculations of low-energy pathways, 3) response to steric interactions, 4) proposed catalytic cycle, 5) interpretation of kinetic data, and 6) rationalization of the enantioselectivity. Unless otherwise stated, the energies in the text are from B3LYP/BS I without zero-point energy corrections.

Initial screening of possible reaction paths

Dichloromethane and dihydride complexes of [Ir(L)]$^+$: Coordination of any reaction component to the naked twelve-electron complex [Ir(L)]$^+$ (Scheme 2) is strongly exothermic.[13] Thus, as cyclooctadiene in the precatalyst is reduced to cyclooctane and released from the catalyst, the free coordination sites created will immediately be reoccupied. The most abundant species in the reaction mixture is the solvent. The coordination of dichloromethane to [Ir(L)]$^+$ is exothermic by 24 kcal mol^{-1}. A second dichloromethane binds more loosely by 7 kcal mol^{-1}. Oxidative addition of H_2 to [Ir(L)]$^+$, which leads to *cis*-dihydrides, is also strongly exothermic with a preference of leaving the position *trans* to phosphorus vacant (34 and 22 kcal mol^{-1}, respectively, always with one hydride in an axial position). The barriers for some oxidative additions of H_2 to Ir^I were found to be very small (1–2 kcal mol^{-1}). Binding of dichloromethane to these dihydride complexes is exothermic by 19 and 24 kcal mol^{-1} for coordination *trans* and *cis* to phosphorus, respectively. Coordination of H_2 instead of a second molecule of dichloromethane is about equally exothermic, again with a slight preference for the neutral ligand in a *trans* position to phosphorus.[14] The energies for these processes are only slightly affected by the increased size of the basis set.

Coordination of substrate alkenes: Alkenes bind strongly to all iridium complexes in this study. Replacement of the dichloromethane in the monosolvated dihydrido–Ir complexes by ethylene to form π complexes **A**–**D** is exothermic by ≈10 kcal mol^{-1}, whereas axial coordination, as in **F**, is exothermic by 5 kcal mol^{-1}. Coordination of additional solvent to the alkene complexes is now exothermic by ≈10 kcal mol^{-1} (Figure 5).

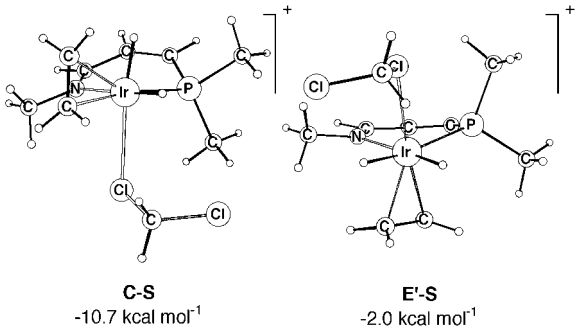

Figure 5. Examples of monosolvated [Ir(H)$_2$(ethylene)] complexes.

The strong binding of alkenes to the catalyst could, in principle, make this step irreversible with the consequence that substrate coordination becomes enantioselective. Indeed, Crabtree has reported an interesting experiment[15] in which first the absolute hydrogenation rates of cyclohexene and 1-methylcyclohexene were measured. In a subsequent competitive experiment, a 1:1 mixture of the olefins was hydrogenated to 50% conversion. The fact that the ratio between the absolute rates (1.2:1) strongly deviates from the result of the competitive experiment (5:1) suggests that the pre-equilibration is slow compared to the overall reaction rate.[16] The strong binding of alkenes is also reflected in the almost zeroth-order dependence on the substrate already reported by Pfaltz.[17] The importance of reversible alkene binding is illustrated by the increased enantioselectivity achieved by lowering the hydrogen pressure, and thus the overall rate of the reaction, reported for a similar type of iridium catalyst.[18]

*Dihydride pathways **A**–**D** and **E'-S***: As seen in Table 1, migratory insertion (MI) taking place in the coordination plane of the ligand is strongly favored (paths **B** and **D**) over MI of the ethylene into an axial Ir–H bond (paths **A** and **C**). It is also evident that the reductive elimination (RE) is rate determining for all paths except for **C**. The most favored path overall is **B**, which occurs with a fast MI (5.6 kcal mol^{-1}) and a

0947-6539/03/0901-0342 $ 20.00+.50/0 *Chem. Eur. J.* **2003**, *9*, No. 1

reasonable barrier for the RE (12.9 kcal mol^{-1}, 8.9 kcal mol^{-1} with coordinated dichloromethane). Also, the formation of alkyl complexes is reversible and a calculated energy of the [Ir(L)(ethane)] complex of 5.6 kcal mol^{-1} suggest that these pathways must somehow be supported by additional solvent, substrate, or dihydrogen in order to proceed. In this context, it is worth mentioning that ethane binds to the iridium catalyst by as much as 15.8 kcal mol^{-1}, although this energy is likely to be somewhat overestimated by a gas-phase calculation. Considering the ability of some iridium complexes to activate alkanes,[19] this strong binding is not unexpected.

It is apparent from the calculations that Ir^{III} is reluctant to coordinate two formally negative ligands in the P-Ir-N plane. This causes the ethylene ligand to migrate to an axial position in the MI in paths **A** and **C**. This phenomenon significantly decelerates these paths. It also renders them less likely to be solvated, since the migration of the alkene and hydride in the transition states will be blocked by an initial axial coordination of solvent. Coordination of a solvent molecule to iridium in the MI of path **C** leads to path **E′-S** (Figure 5). The result is a remarkably strong stabilization (15 kcal mol^{-1}); however, this disappears in the reductive elimination in which solvent coordination is lost.

In an attempt to stabilize the transition state for reductive elimination in paths **B** and **D**, a dichloromethane molecule was allowed to coordinate to iridium. The conclusion that could be drawn from this experiment is that the stabilization is rather weak ($\approx$4 kcal mol^{-1}). In the real catalysts, axial coordination of solvent will be considerably weaker as a result of the steric requirements of both the *tert*-butyl group of the oxazoline and the aryl groups of the phosphine moiety. Thus, to bring to a close the discussion about solvation, we would like to state that solvent coordination to iridium is certainly strong in some complexes, but the effects on relative rates of different reaction paths are much smaller. However, as noted early on by Crabtree, the hydrogenation reaction is strongly repressed by coordinating solvents.

*Tetrahydride pathways **A**-H_2 to **F**-H_2*: The seemingly problematic endothermicity of the steps described above suggests that the iridium atom is still too unsaturated. Therefore, we began a search for alternative pathways with H_2 instead of solvent to fill up the sixth coordination site in the octahedral Ir^{III} complexes. The question to be answered was whether other reaction channels could be opened by addition of this second molecule of H_2 (paths **A**-H_2 to **G**-H_2). In fact, polyhydrides have been suggested as intermediates in the hydrogenation of pinenes by Crabtree's catalyst.[20]

In the calculations, the binding of H_2 to the dihydrido ethylene complexes was exothermic by $\approx$10 kcal mol^{-1}. However, replacing a solvent molecule by H_2 is only slightly exothermic (e.g., 1 kcal mol^{-1} for path **C**). In terms of free energy, this binding thus seems to be endergonic and pressure effects on the reaction outcome are easily envisioned. According to calculations on path **C**-H_2, the activation energy for an associative solvent displacement by H_2 is 6 kcal mol^{-1}. The H–H bond in the Ir–H_2 complexes is activated and the bond length is found to be approximately 0.81–0.88 Å, depending on the structure. For the [Ir(H)$_2$(ethylene)(H_2)] complexes (**2**) in paths **A**-H_2 and **C**-H_2, facile oxidative additions to yield formal Ir^{V} tetrahydrides were found (resulting in paths denoted **A′**-H_2 and **C′**-H_2). The potential energy surfaces of the dihydrogen-assisted paths **A**-H_2 to **D**-H_2 are shown in Figure 6.

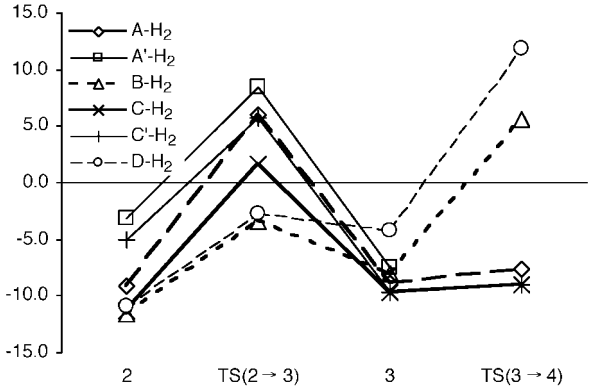

Figure 6. Potential energy surfaces of paths **A**-H_2 to **D**-H_2 (B3LYP/BSI, kcal mol^{-1}).

It can also be seen in Figure 6 that the MI step in paths **B**-H_2 and **D**-H_2 is still the most facile by far and the activation energies measured from the corresponding Ir–ethylene complexes are only slightly changed (Table 1). However, most remarkably, the MI in the H_2-assisted path **C**-H_2, is accomplished by means of a concerted oxidative addition of H_2 to form an [Ir^{V}(H)$_3$(ethyl)] complex (Figure 7). While paths **B**-H_2 and **D**-H_2 are effectively blocked by high activation energies of the RE (**TS$_{(3\rightarrow4)}$**), the Ir–ethyl complex of path **C**-H_2 undergoes this step with a negligible barrier of only 0.6 kcal mol^{-1} relative to the corresponding Ir–ethyl complex. It should be noted that the RE in paths **B**-H_2 and **D**-H_2 are accompanied by a concerted oxidative addition of H_2 resulting in catalytic cycles with a *constant* formal oxidation state of III on the metal (Figure 7).

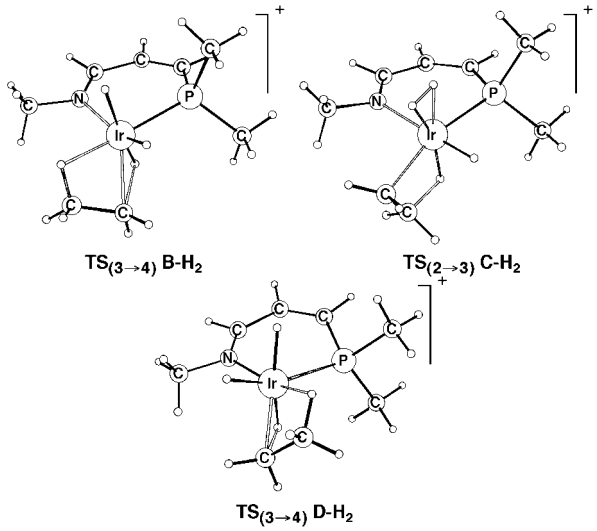

Figure 7. Oxidative addition of H_2 coupled with migratory insertion and reductive elimination.

  0947-6539/03/0901-0343 $ 20.00+.50/0

We now turn our attention to H_2-activation of paths **E**, **E′**, **F**, and **F′**. With an axially coordinated substrate, four different migratory insertion pathways could be envisioned. The MI could take place *cis* or *trans* to phosphorus with the H_2 molecule *cis* or *trans* to the olefin. The calculations indicated that keeping a *cis* relationship between the olefin and the H_2 (**E**-H_2 and **F**-H_2) is very unfavorable in the MI and path **F**-H_2 is further blocked by the non-existence of the corresponding alkyl complex. Activation of the [Ir(H)$_2$H$_2$(ethylene)] by a facile isomerization (an activation energy of 5.6 kcal mol^{-1} was found for this step) [21] to put both hydrides in the coordination plane of the ligand dramatically lowered the MI barrier to only 8.4 kcal mol^{-1} relative to the corresponding olefin complex (path **E′**-H_2). However, this pathway is hampered by a significantly higher barrier for the RE (12.6 kcal mol^{-1} using the same reference). At this point, the difference in absolute energy between the MI barrier in path **C**-H_2 and the RE in path **E′**-H_2 is only 2 kcal mol^{-1} in favor of path **C**-H_2.

Estimation of relative rates: In a catalytic system with more than one rate-determining transition state, working out the kinetics will provide a means to differentiate between mechanistic alternatives. To determine which paths to pursue, we made some initial assumptions. Starting from a common resting state, the intermediate iridium–alkyl complex (**3**) could be formed by coordination of substrate and H_2, followed by a migratory insertion of the olefin into an Ir–H bond. This iridium–alkyl intermediate could thereafter either revert to the resting state of the catalyst or proceed over the next barrier, the reductive elimination, and irreversibly form the hydrogenated product (Figure 2). The result from this analysis is reported in Table 1 as the logarithm of the ratio between the calculated rate constant (k_{tot}) and k_{tot} for path **A**. It is evident from Table 1 that pathways **E′-S**, **A**-H_2 to **C**-H_2, and **E′**-H_2 require more attention.

More accurate calculations of low-energy pathways: Basis set deficiencies could be one source of error that lead to incorrect conclusions. We therefore used an extended basis set (see Computational Methods for details) to evaluate this effect and the results are reported in Table 2. Most encouragingly, the changes in relative energies are small, and the trend is towards energies being moved slightly apart.

The relative rates were reanalyzed, as described above, but with the free energies this time (Figure 8): the preference for path **C**-H_2 increased. The second most likely reaction mechanism is still path **E′**-H_2. In the real catalyst, the two phenyl groups or *o*-tolyl groups on phosphorus are expected to add steric interactions between the substrate and the catalyst in paths **A**, **A**-H_2, **B**, and **B**-H_2, further destabilizing these paths.

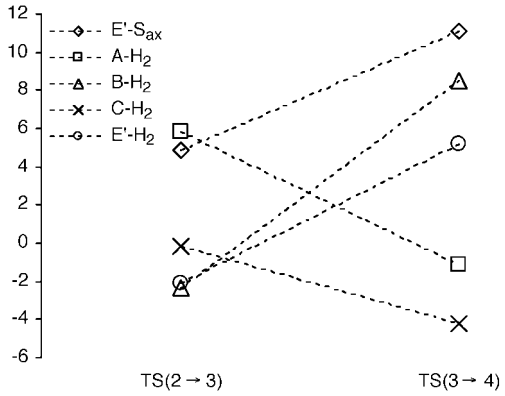

Figure 8. Relative activation free energies of migratory insertion and reductive elimination calculated at B3LYP/BS II//B3LYP/BS I (kcal mol^{-1}).

Response to steric interactions: To differentiate further between the two remaining mechanistic alternatives, additional calculations were performed with 2-methyl-2-butene as the substrate. In this case, the migratory insertion in path **C**-H_2 was compared to the reductive elimination in path **E′**-H_2 (Figure 9). Again, there is an increase in the energy difference in favor of path **C**-H_2. At B3LYP/BS I, the difference in energy between the two transition states is increased from 1.8 to 8.1 kcal mol^{-1}. Apparently, path **E′**-H_2 is much more responsive to steric hindrance. Single-point calculations with BS II leads to a preference for path **C**-H_2 by as much as 9.3 kcal mol^{-1}. Addition of thermal corrections to enthalpy and free energy further increases the preference to 11.1 and 12.2 kcal mol^{-1}, respectively. Thus, path **C**-H_2 is the reaction mechanism very much favored by our DFT calculations.

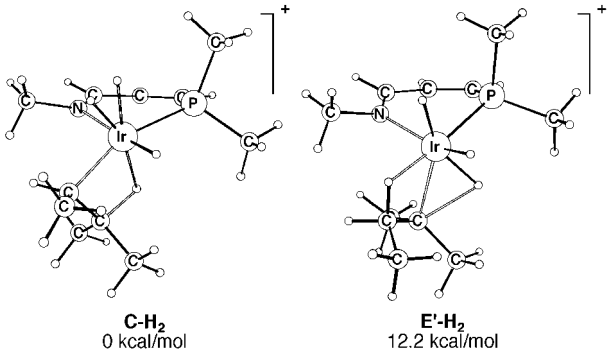

Figure 9. Rate-limiting transition states in path **C**-H_2 (**TS$_{(2-3)}$**) and **E′**-H_2 (**TS$_{(3-4)}$**). Relative free energies from B3LYP/BS II//B3LYP/BS I in kcal mol^{-1}.

Proposed catalytic cycle: Based on our extensive calculations, we propose the reaction mechanism depicted in Scheme 5 to be operative in the hydrogenation of alkenes with

Table 2. Energies and free energies [kcal mol^{-1}] derived from B3LYP/BS II//B3LYP/BS I.[a]

Path	**2**		TS$_{(2-3)}$		**3**		TS$_{(3-4)}$		log(rel. rate)[b]
E′-S	2.1		3.2	4.9			10.1	11.1	0.0
A-H_2			4.6	5.9			−3.0	−1.1	3.8
B-H_2			−3.2	−2.4			5.3	8.5	1.9
C-H_2	−11.9	−9.7	−1.3	−0.1	−6.7	−2.4	−6.7	−4.2	8.3
E′-H_2			−2.7	−2.1			2.6	5.2	4.3

[a] Energies are listed in the left columns and free energies to the right. [b] Relative rates based on free energies. The underlying mechanistic basis assumes a common resting state of the catalyst, a semireversible formation of the Ir–ethyl complex **3** present in a steady-state concentration, and an irreversible reductive elimination.

0947-6539/03/0901-0344 $ 20.00+.50/0 *Chem. Eur. J.* **2003**, *9*, No. 1

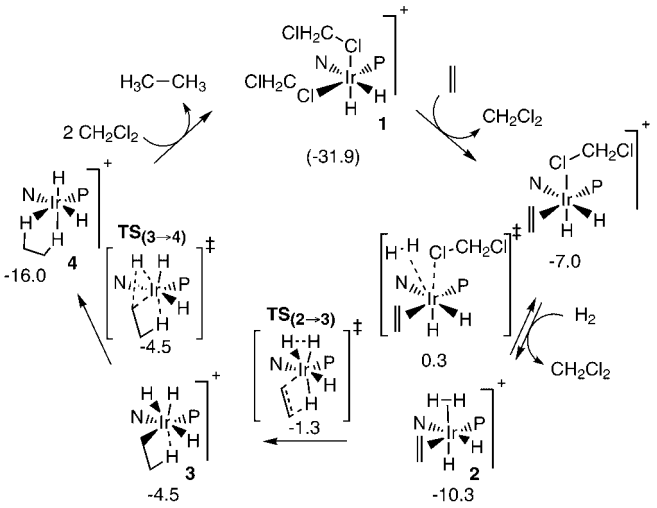

Scheme 5. Proposed catalytic cycle and enthalpies (B3LYP/BS II//B3LYP/BS I, kcal mol^{-1}) for the iridium–phosphanooxazoline-catalyzed hydrogenation of unfunctionalized olefins. The energy in parenthesis gives the driving force for the reduction of ethene by H_2.

[Ir(PN-ligand)(cod)] catalyst precursors. This cycle starts with the most stable Ir^{III}–dihydride complex found in the study. In two consecutive steps, an olefin is coordinated *trans* to phosphorus and in an endergonic step, an H_2 is coordinated in the remaining axial position. The coordination of H_2 might be either dissociative, with an energy cost of the iridium–dichloromethane bond, or associative, as shown in Scheme 5. The olefin in this complex can then undergo a migratory insertion into the axial Ir–H bond, a reaction that occurs simultaneously with an oxidative addition of H_2. The resulting Ir^{V} species is now extremely labile and the reductive elimination occurs with a negligible barrier.

The catalysis is thus taking place without the intervention of Ir^{I} in any step, in contrast to the analogous rhodium systems in which the oxidation state of the metal changes between I and III.[22] The strong binding of alkenes to iridium should be reflected in the kinetic measurements as a zeroth-order dependence on alkene concentration; in other words, the resting state of the catalyst will contain one bound alkene. The rate-determining step is either the coordination of H_2 or the migratory insertion.

Interpretation of kinetic data: In the kinetic part of this work, we have confirmed the results previously reported by Pfaltz and co-workers, that the reaction rate is independent of the alkene concentration[17] (in the concentration range 0.125–0.500 M, 10 bar hydrogen pressure). This indicates a reaction mechanism in which the coordination of alkene to the catalyst is not rate determining. As indicated by the DFT calculations, binding of ethylene to **1** by displacement of a solvent molecule is exothermic ($\Delta H = -7.0$ kcal mol^{-1}, B3LYP/BS II//B3LYP/BS I). This exothermicity, in combination with the zeroth-order dependence on alkene concentration, suggests that the catalyst coordinates an alkene in the resting state.

According to the kinetic measurements, the reaction is first order in hydrogen pressure. This could mean one of two things: the reaction between the catalyst in the resting state and H_2, by ligand displacement, is rate determining,[22] or the coordination of H_2 is endergonic. According to the calculations, the displacement of one dichloromethane in the monosolvated [Ir(H)$_2$(ethylene)] complexes by H_2 is only weakly exothermic, an exothermicity that could easily be outbalanced by the difference in activity between H_2 and dichloromethane. Thus, the calculations offers two alternative explanations for the first-order dependence on H_2.

As expected, the reaction is first order with respect to catalyst concentration. Thus, reversible dimerization of the catalyst does not seem to be of importance.

Rationalizing the enantioselectivity: To create a model for the enantioselectivity-determining step, calculations were performed on the full-sized Pfaltz' catalyst (R = *t*Bu, Ar = Ph, Scheme 1) with (*E*)-1,2-diphenylpropene as the substrate. The first thing to notice in Figure 10 is the perfect matching of

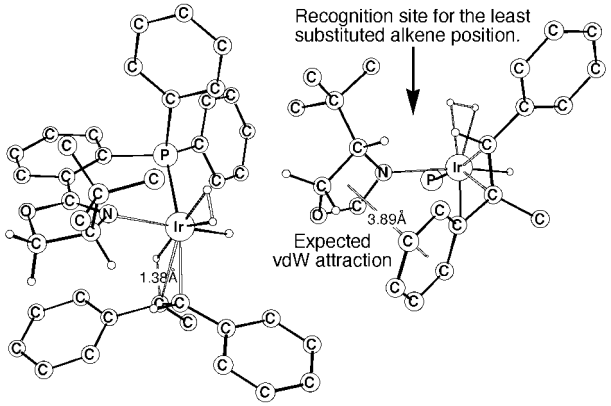

Figure 10. Transition state of the migratory insertion $\mathbf{TS}_{(2\rightarrow3)}$ in path **C**-H_2 for the real catalyst and substrate use in the kinetic study (left). Selectivity model based on the alkene complex **2** of path **C**-H_2 (right).

shapes between the catalyst and the substrate in the Ir–alkene complex **2**. The *tert*-butyl group serves to recognize the unsubstituted position of the alkene, and the oxazoline ring is stacked on top of one of the phenyl groups of the substrate. This explanation is in agreement with the better performance of *neo*-pentyl-substituted phosphanooxazoline in combination with tetrasubstituted alkenes, such as *trans*-α,α,β-trimethylstyrene.[1]

Coordination of alkene to the catalyst **1** is exothermic, according to the calculations on the small model system ($\Delta E = -10.7$ kcal mol^{-1}, B3LYP/BS I). Considering the increased steric demands of both the catalyst and the substrate, this step could be assumed to be considerably less favored. Calculations on the full catalysts and (*E*)-1,2-diphenylpropene shows that this step occurs with rather small steric interactions and the alkene binding slightly weakened ($\Delta E = -6.1$ kcal mol^{-1}, B3LYP/LACVP). Dispersion interactions, not taken into account by the B3LYP calculations, will make the alkene coordination stronger. Since the kinetic investigations indicate that the substrate coordination step is not rate limiting, this suggests an exothermic, but possibly reversible formation of Ir–alkene complexes, and the final enantioselectivity will be determined as a combination of the stabilities

of the different olefin complexes and the MI step. For path **C**-H_2, both effects are expected to work in the same direction.

Double bond migration has been observed for some substrates in iridium-catalyzed alkene hydrogenations.[4d, 20, 23] This process will add difficulties to the design of new ligands for this reaction, as pointed out in a recent article by Burgess and co-workers.[23]

Conclusion

In this mechanistic study of the iridium–phosphanooxazoline-catalyzed hydrogenation of unfunctionalized olefins, we have been able to propose a detailed reaction mechanism that is dramatically different from other related catalytic systems. The computational study has shown that the oxidative addition of H_2 not only to Ir^I but also to Ir^{III} is facile and that the corresponding iridium–hydrogen/hydride complexes of different configurations are likely to be in rapid equilibrium. We have also discovered an unusual acceleration of both migratory insertion and reductive elimination steps, caused by a simultaneous oxidative addition of H_2. In case of the coupled reductive elimination/oxidative addition, the metal is in the catalytic cycle in a *constant* oxidation state of III. In the other case, in which migratory insertion is coupled to oxidative addition of H_2, the metal is cycled between Ir^{III} and Ir^V, a fact that greatly lowers the activation energy for the final step of the reaction, the reductive elimination of an alkane.

The kinetic experiments have shown that the reaction is zeroth order with respect to the alkene concentration. We interpret this as an indication of a resting state of the catalyst to which the alkene is already bound. This is supported by the computational data which states that alkene binding to iridium is relatively strong compared to solvent coordination. Not surprisingly, the reaction is first order with respect to the catalyst concentration. We have also found that the reaction is first order with respect to the hydrogen pressure. We favor the interpretation that the coordination of H_2 to the catalyst is endergonic, which is supported by the calculations and the fact that the solvent concentration is much higher compared to the H_2 concentration. However, the alternative that H_2 coordination by ligand displacement is rate determining is supported by the calculations on the sterically less-hindered model system.

A possible catalytic Ir^{III}–Ir^V cycle involving a coupled migratory insertion of the alkene into an Ir–H bond and oxidative addition of H_2, resulting in a very labile Ir^V species, is suggested to be the mechanism of the reaction. This mechanism is shown to be compatible with the observed enantioselectivity of the reaction. The mechanism also explains the preferred ligand substitution for tetrasubstituted alkenes and gives a reason for the usually improved performance of *o*-tolyl-substituted phosphanes.

Experimental Section

The reaction studied experimentally is depicted in Scheme 6. All hydrogenation reactions were carried out on a computer-controlled Endeavor Catalyst screening system.[10] (*E*)-1,2-Diphenylpropene was purchased from Aldrich and used as received. CH_2Cl_2 was distilled from CaH_2 directly prior to use. Catalyst and substrate were prepared as standard solutions under argon in dry CH_2Cl_2. The catalyst was prepared according to a literature procedure[1] from (4*S*)-4-*tert*-butyl-2-(2-diphenylphosphinophenyl)-1,3-oxazoline,[11] [{Ir(cod)Cl}$_2$] (Johnson Mathew) and NaBARF·3 H_2O.[12]

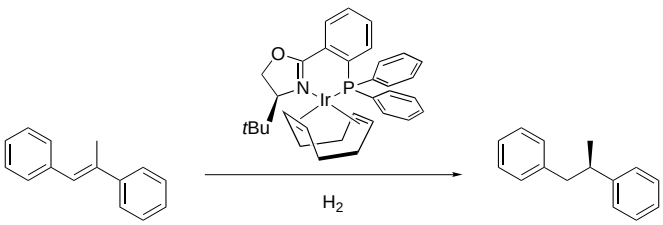

Scheme 6. System studied by kinetic measurements.

Typical kinetic measurement procedure: The instrument was fitted with 8 glass liners (acid-cleaned (conc. HNO_3) and dried) and then sealed. 1.00 mL of substrate solution in CH_2Cl_2 was added to each vessel through the syringe port. Vessels were purged three times with Ar (5 atm), and then the catalyst solution was added through the syringe ports. Total reaction volumes in all cases were 2.0 mL. The reaction vessels were stirred at 700 rpm and pressurized with H_2 to the working pressure. Data acquisition was started individually when each vessel reached the pre-set pressure. All reactions were run in duplicate. After complete conversion, the reaction vessels were opened and the reaction solutions were filtered through Pasteur pipettes filled with silica to remove catalyst residues. The product and any unreacted substrate were eluted with diethyl ether/pentane 1:1. The solvent was evaporated and the residue redissolved in *n*-hexane for HPLC analysis. Conversion and enantiomeric excess (*ee*) were determined by HPLC (Chiracel OJ, *i*PrOH/*n*-hexane 1:99) $R_t = 12.3$ min (major enantiomer) *R*, 16.5 min (minor enantiomer) *S*, 24.9 min (substrate) on a Gilson 322 instrument, detection at $\lambda = 254$ nm. Conversions were calculated from a calibrated standard plot of relative absorbances of product and substrate. In all cases, conversions were in the order of 60–95%. In the calculation of rate constants, the first third of the kinetic traces were used. *Ee*'s were in range of 89–91% of (*R*) as major enantiomer.

Acknowledgements

This work was supported by the Swedish Natural Science Research Council (NFR), the Foundation for Strategic Research (SSF), and the Swedish Research Council for Engineering Sciences (TFR). Access to supercomputer time was provided by the Swedish Council for High Performance Computing (HPDR) and Parallelldatorcentrum (PDC), Royal Institute of Technology.

[1] A. Lightfoot, P. Schnider, A. Pfaltz, *Angew. Chem.* **1998**, *110*, 3047; *Angew. Chem. Int. Ed.* **1998**, *37*, 2897.
[2] R. Hilgraf, A. Pfaltz, *Synlett* **1999**, 1814.
[3] R. Crabtree, *Acc. Chem. Res.* **1979**, *12*, 331 and references therein.
[4] a) R. H. Crabtree, H. Felkin, G. E. Morris, *J. Chem. Soc. Chem. Commun.* **1976**, 716; b) W. J. Hälg, L. R. Öhrström, H. Rüegger, L. M. Venanzi, *Magn. Res. Chem.* **1993**, *31*, 677; c) T. W. Brauch, C. R. Landis, *Inorg. Chim. Acta* **1998**, *270*, 285;. d) B. F. M. Kimmich, E. Somsook, C. R. Landis, *J. Am. Chem. Soc.* **1998**, *120*, 10115.
[5] a) A. D. Becke, *J. Chem. Phys.* **1993**, *98*, 5648; b) C. Lee, W. Yang, R. G. Parr, *Phys. Rev. B* **1988**, *37*, 785.
[6] M. J. Frisch, G. W. Trucks, H. B. Schlegel, G. E. Scuseria, M. A. Robb, J. R. Cheeseman, V. G. Zakrzewski, J. A. Montgomery, Jr., R. E. Stratmann, J. C. Burant, S. Dapprich, J. M. Millam, A. D. Daniels, K. N. Kudin, M. C. Strain, O. Farkas, J. Tomasi, V. Barone, M. Cossi, R. Cammi, B. Mennucci, C. Pomelli, C. Adamo, S. Clifford, J. Ochterski, G. A. Petersson, P. Y. Ayala, Q. Cui, K. Morokuma, D. K. Malick, A. D. Rabuck, K. Raghavachari, J. B. Foresman, J. Cioslowski, J. V.

  0947-6539/03/0901-0346 $ 20.00+.50/0

Ortiz, B. B. Stefanov, G. Liu, A. Liashenko, P. Piskorz, I. Komaromi, R. Gomperts, R. L. Martin, D. J. Fox, T. Keith, M. A. Al-Laham, C. Y. Peng, A. Nanayakkara, C. Gonzalez, M. Challacombe, P. M. W. Gill, B. Johnson, W. Chen, M. W. Wong, J. L. Andres, C. Gonzalez, M. Head-Gordon, E. S. Replogle, J. A. Pople, Gaussian 98, Revision A.3, Gaussian, Pittsburgh, PA, **1998**.

[7] a) P. J. Hay, W. R. Wadt, *J. Chem. Phys.* **1985**, *82*, 285; b) P. J. Hay, W. R. Wadt, *J. Chem. Phys.* **1985**, *82*, 299.

[8] D. Andrae, U. Häussermann, M. Dolg, H. Stoll, H. Preuss, *Theor. Chim. Acta* **1990**, *77*, 123.

[9] Jaguar 4.0, Schrödinger, Portland, OR, **1991–2000**.

[10] More information can be obtained from the website http://www.argotech.com/Endeavor.

[11] J. V. Allen, G. J. Dawson, C. G. Frost, J. M. J. Williams, *Tetrahedron* **1994**, *50*, 799.

[12] H. Nishida, N. Takada, M. Yoshimura, T. Sonoda, H. Kobayashi, *Bull. Chem. Soc. Jpn.* **1984**, 57, 2600.

[13] The energy of this species is 63.0 kcal mol^{-1} relative to **1** at B3LYP/BSI.

[14] This is in agreement with the experimental results reported by Crabtree and Uriarte for the oxidative addition of H_2 to $[Ir(COD)(PCy_3)(py)]^+$: R. H. Crabtree, R. J. Uriarte, *Inorg. Chem.* **1983**, *22*, 4152.

[15] R. H. Crabtree, H. Felkin, G. E. Morris, *J. Organomet. Chem.* **1977**, *141*, 205.

[16] For a discussion of the original experiment, see: R. H. Crabtree, P. C. Demou, D. Eden, J. M. Mihelcic, C. A. Parnell, J. M. Quirk, G. E. Morris, *J. Am. Chem. Soc.* **1982**, *104*, 6994.

[17] D. G. Blackmond, A. Lightfoot, A. Pfaltz, T. Rosner, P. Schnider, N. Zimmermann, *Chirality* **2000**, *12*, 442.

[18] J. Blankenstein, A. Pfaltz, *Angew. Chem.* **2001**, *113*, 4577; *Angew. Chem. Int. Ed.* **2001**, *40*, 4445.

[19] See, for example: R. H. Crabtree, *Organometallic Chemistry of the Transition Metals*, 2nd ed., Wiley, New York, **1994**, pp. 321–326; S. Niu, M. B. Hall, *J. Am. Chem. Soc.* **1999**, *121*, 3992.

[20] J. M. Brown, A. E. Derome, G. D. Hughes, P. K. Monaghan, *Aust. J. Chem.* **1992**, *45*, 143.

[21] The reaction takes place with a "trihydrogen anion" transition state. See also: S. Li, M. B. Hall, J. Echert, C. M. Jensen, A. Albinati, *J. Am. Chem. Soc.* **2000**, *122*, 2903.

[22] C. R. Landis, P. Hilfenhaus, S. Feldgus, *J. Am. Chem. Soc.* **1999**, *121*, 8741.

[23] D.-R. Hou, J. Reibenspies, T. J. Colacot, K. Burgess, *Chem. Eur. J.* **2001**, *7*, 5391.

Received: July 1, 2002 [F4218]

  0947-6539/03/0901-0347 $ 20.00+.50/0